Pyrolysis of LignoBoost lignin in $ZnCl_2$-KCl-NaCl molten salt media

Genuino, Homer C.; Contucci, Ludovico; Velasco, Jessi Osorio; Sridharan, Balaji; Wilbers, Erwin; Akin, Okan; Winkelman, Josef G. M.; Venderbosch, Robertus H.; Heeres, Hero J.

Published in:
Journal of Analytical and Applied Pyrolysis

DOI:
10.1016/j.jaap.2023.106005

Publication date:
2023

Journal of Analytical and Applied Pyrolysis 172 (2023) 106005

Contents lists available at ScienceDirect

Journal of Analytical and Applied Pyrolysis

journal homepage: www.elsevier.com/locate/jaap

Pyrolysis of LignoBoost lignin in $ZnCl_2$-KCl-NaCl molten salt media: Insights into process-pyrolysis oil yield and composition relations

Homer C. Genuino [a], Ludovico Contucci [a], Jessi Osorio Velasco [a], Balaji Sridharan [a], Erwin Wilbers [a], Okan Akin [a], Josef G.M. Winkelman [a], Robertus H. Venderbosch [b], Hero J. Heeres [a,*]

[a] Department of Chemical Engineering, Engineering and Technology Institute Groningen (ENTEG), University of Groningen, Nijenborgh 4, 9747 AG Groningen, the Netherlands

[b] BTG Biomass Technology Group B.V., Josink Esweg 34, 7545 PN Enschede, the Netherlands

ARTICLE INFO

Keywords:
Biomass
Lignin
Pyrolysis
Molten salts
Depolymerization
Demethoxylation

ABSTRACT

Depolymerization of lignin by pyrolysis has been identified as a viable route to produce renewable fuels and biobased platform chemicals. Herein we report the pyrolysis of LignoBoost lignin in a molten salt consisting of $ZnCl_2$-KCl-NaCl (60:20:20 mol ratio) in a g-scale reactor set-up with a focus on the liquid phase yields and composition. The effects of relevant process parameters such as temperature (250–450 °C), reaction time (10–50 min), and N_2 flow rate (10–30 mL min^{-1}) on the product yields were elucidated using design of experiments. The highest bio-oil yield was 47.1 wt% (450 °C, 10 min) and the yield of organics in the bio-oil at this condition was 24 wt% (on lignin intake), the remainder being water. The latter is considerably higher than found for an experiment at similar conditions without salt (16 wt%). Temperature and reaction time were shown to have the largest effects on bio-oil yield. Prolonged reaction times resulted in higher amounts of gas phase components (H_2, CO_2) and water, and a reduced amount of solid products. Statistical analyses and validation experiments showed that the experimental product yields are in good agreement with the predicted values from the model. The properties and molecular composition of the liquid products were determined using various analytical techniques and reveal that the presence of a molten salt during pyrolysis has a positive influence on the composition of the liquid phase like a higher level of depolymerization and higher selectivity to aromatic and phenolic monomers compared to thermal pyrolysis.

1. Introduction

Lignin is a promising feed to produce biofuels and biobased chemical commodities [1]. The pulp and paper industry [2] produces large amounts of lignin containing residues with production levels exceeding 40–50 million tons per year [3]. These are currently mainly used to fulfill the energy requirements in the process [4]. However, these residues have high potential for higher-value applications like the use as a feed for green chemical building blocks. From a chemical perspective, the major hurdle associated with lignins from the paper and pulp industry is their highly condensed structure, which is recalcitrant toward catalytic depolymerization.

Valorization routes for lignin are considerably less developed than for the (hemi)cellulose fraction of lignocellulosic biomass. Nevertheless, (thermo)chemical conversion approaches such as pyrolysis, gasification, hydrogenolysis, liquefaction, and oxidation, have been reported for lignin depolymerization [5,6]. Among these strategies, pyrolysis has been widely applied to produce a liquid product known as pyrolysis liquid or bio-oil, which is potentially a more valuable product than the starting lignin [7]. During pyrolysis of lignin, the structure is depolymerized into smaller molecules such as aromatic and phenolic monomers as well as oligomers. The bio-oils can be further upgraded in subsequent processing steps to extend their application range [7]. Several pyrolysis technologies (i.e., grinding, microwave, and stepwise pyrolysis) have been developed [8,9]. However, the liquid yields for lignin pyrolysis in lab scale set-ups (typically < 25 wt%) are generally much lower than for lignocellulosic biomass pyrolysis (up to 70 wt%) and are depending on the type of lignin [10]. Fast pyrolysis is favored

* Corresponding author.
E-mail address: h.j.heeres@rug.nl (H.J. Heeres).

https://doi.org/10.1016/j.jaap.2023.106005
Received 28 December 2022; Received in revised form 5 May 2023; Accepted 8 May 2023
Available online 9 May 2023

Table 1
List of reported eutectic compositions of halide-based molten salts for the thermal processing of biomass.

Molten salts	Molar ratio	Melting point (°C)	Reference
$AlCl_3$-KCl	67:33	128	[22]
$AlCl_3$-NaCl	55:45	133	[22]
CuCl-KCl	65:35	150	[16,22]
$ZnCl_2$-KCl-LiCl	40:20:40	240	[22]
KCl-LiCl-NaCl	36:55:9	346	[22]
$ZnCl_2$-KCl	70:30	262	[13–16,22]
$ZnCl_2$-NaCl	70:30	255	[22]
$ZnCl_2$-KCl-CuCl	48.1:41.1:10.8	190	[16,22]
LiF-NaF-KF	46.5:11.5:42	454	[18,19,21]
$ZnCl_2$	-	283	[16,22]
$ZnCl_2$-KCl-NaCl (this work)	60:20:20	203	-

- not applicable

over slow pyrolysis when aiming for maximizing the conversion of lignin into liquids [5].

A promising upcoming pyrolysis technology involves the use of molten salts in the pyrolysis section. Various molten salt combinations are available and may be used [11–22]. The molten salts can i) act as a solvent or a dispersing agent to transfer the biomass to the pyrolysis reactor, which particularly facilitates lignin feeding and ii) may also act as a catalyst and change the liquid product composition. So far, halide based molten salts have gained the highest attention [13–16, 22] and examples of such halide mixtures and their melting points are listed in Table 1. From this group, particularly the chlorides show interesting properties a.o. low melting points, which may be tailored depending on their composition.

Pyrolysis of lignocellulosic biomass in the presence of molten salts has been reported and relevant details about these studies (selected) are summarized in Table 2 [15–26]. Typically, the product selectivity changes considerably when salts are present during pyrolysis, and particularly in the case of lignocellulosic biomass. Here acetic acid and furfural are being formed in high amounts. The liquid yields are also affected, though the actual effect is not yet clear, and both reductions and higher yields have been reported when compared to pyrolysis in the absence of salts. For example, Jiang et al. [16] investigated the effects of pyrolysis parameters and composition of $ZnCl_2$-based molten salts on product yields and the composition of the bio-oils derived from cellulose and rice husk. For cellulose, the liquid yield was 61.8 wt%, though the organic content was very low (11.6 wt%) yields. Adding CuCl (a reducing additive) to the $ZnCl_2$-KCl couple gave a significant improvement and the water content decreased from 46 % to 21 %, whereas the total liquid yield was about the same. The optimal temperature for cellulose pyrolysis was found to be about 530 °C, giving a bio-oil yield of almost 35 wt%, though almost half of it was water [16].

In another study, Dutta et al. [22] reported the slow pyrolysis of sawdust in chloride-based molten salts at relatively mild pyrolysis conditions (about 400 °C, 1 atm). The highest bio-oil yield was 66 wt% using $ZnCl_2$-KCl-LiCl, which is significantly higher than the yield without the molten salts (32 wt%). We recently reported research to convert woody biomass to a liquid hydrocarbon product using molten salt slow pyrolysis ($ZnCl_2$-NaCl-KCl at 60:20:20 mol ratio), followed by a subsequent catalytic hydrotreatment of the pyrolysis liquids to hydrocarbons [25]. The pyrolysis process resulted in a liquid yield of 46 wt% and analyses showed that the liquid was highly enriched in furfural and acetic acid. Recently, molten salt pyrolysis ($ZnCl_2$-NaCl-KCl) of biomass using a micro-pyrolyzer coupled with GC-MS was reported [26]. It was observed that the salts have a major catalytic effect on the pyrolysis volatiles when compared to those from pyrolysis without salts. Molten salt pyrolysis of Lignoboost Kraft lignin selectively produced guaiacol and syringol, whereas cellulose, pinewood, and wheat straw produced mostly furfural and acetic acid. The yields of volatiles from all lignocellulosic feedstock was less in the presence of chloride molten salts, though this finding needs further validation using calibration curves. Nevertheless, these recent studies on molten salt pyrolysis of lignocellulosic biomass (Table 2) show that Zn based chloride salts may act as a catalyst during pyrolysis.

Despite the potential of molten salts for biomass pyrolysis, research on the pyrolysis particularly of lignin in molten salt media has received

Table 2
Literature overview of research on the pyrolysis of lignocellulosic biomass and lignins in chloride-based molten salt.

Biomass	Molten salts (mol%)	Molar ratio (mol/mol)	Temperature (°C)	Yield (wt%)			Major compounds identified in bio-oil	Ref.
				Bio-oil	Water	Total liquid[a]		
Cellulose	$ZnCl_2$-KCl	53.8:46.2	450	11.6	50.0	61.8	Mainly 2-methoxy furan. Others: 3-methyl furan, acetylfuran, aldonolactone derivative, D-xylopyranose derivative	[16]
	KCl-CuCl	66:34	450	11.8	21.0	32.8	Not reported	
	$ZnCl_2$	Not applicable	450	35.0	46.0	81.0	Not reported	
Sawdust	CuCl-KCl	65:35	350	Not reported	Not reported	41	Mainly acetic acid and furfural	[22]
	CuCl-KCl	65:35	450	Not reported	Not reported	63		
	$ZnCl_2$-KCl-LiCl	40:20:40	350	Not reported	Not reported	50		
	$ZnCl_2$-KCl-LiCl	40:20:40	450	Not reported	Not reported	58		
	$ZnCl_2$-KCl-NaCl	60:20:20	400	-	-	47		
	None		350	Not reported	-	19	Mainly acetic acid and furfural. Others: hydroxyacetone, methyl ester acetic acid, propanic acid, 1-hydroxy-2-butanone, 4-methyl guaiacol, acetyl furan	
Pine-wood	$ZnCl_2$-KCl-NaCl	44.3: 41.9: 13.9	350	Not reported	Not reported	Not reported	Acetic acid and furfural	[26]
		60:20:20	450	Not reported	Not reported	46	Acetic acid and furfural	[25]
Kraft lignin	$ZnCl_2$-KCl	53.8:46.2	550	29[b]	14	43[b]	Mainly guaiacol, o-/m-/p-cresol, and methanol. Others: o-/m-/p ethylphenol, phenol, 4-ethyl guaiacol, catechol, 4-methylcatechol, syringol	[15]

[a]Sum of bio-oil and water yields.
[b]Determined by difference from the yields of char, water, and gases.

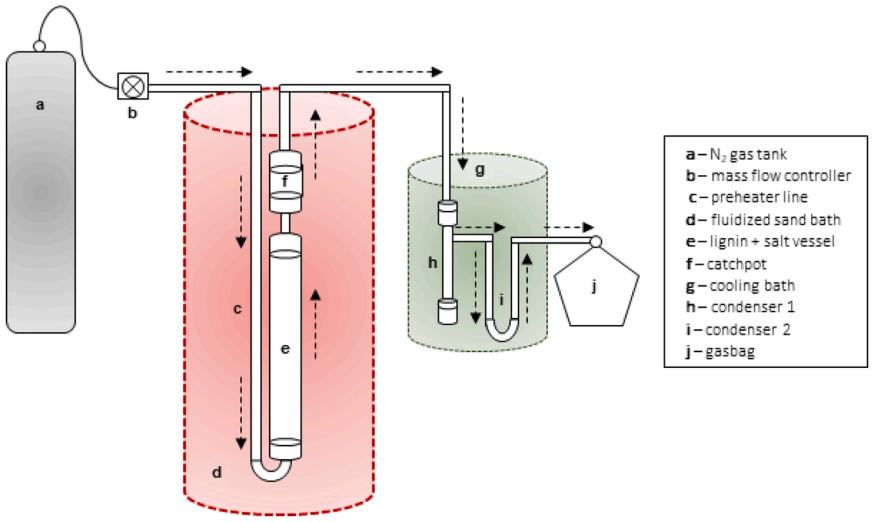

Fig. 1. Schematic diagram of the gram scale reactor setup for the pyrolysis of LignoBoost lignin in molten salts ($ZnCl_2$-KCl-NaCl at 60:20:20 mol ratio).

Table 3
Two-level three-factor fractional factorial design matrix used to study the effects of process parameters for the pyrolysis of LignoBoost lignin in molten salts ($ZnCl_2$-KCl-NaCl at 60:20:20 mol ratio) on bio-oil, organics in bio-oil, solid, and gas yields (average).

Temperature (°C)	Reaction time (min)	N_2 flow rate (mL min^{-1})	Bio-oil yield (wt%)	Organics yield (wt %)	Solid yield (wt%)	Gas yield (wt %)
450	50	30	42.7	n.d.	41.0	16.2
450	50	30	40.8	11.7	41.7	17.5
250	50	30	28.8	9.9	69.5	1.7
250	10	10	6.3	0	92.0	1.8
250	10	10	7.0	0	91.3	1.7
350	30	20	25.7	n.d.	64.0	10.3
250	50	30	28.0	6.9	70.1	1.9
350	30	20	40.0	13.6	56.4	3.6
450	10	30	33.6	11.1	40.9	25.5
250	50	30	24.3	n.d	74.8	1.0
250	10	30	5.3	0	87.7	7.0
450	50	10	35.5	15.5	44.9	19.6
350	30	20	33.3	7.3	48.0	18.6
450	50	10	36.8	15.6	35.8	27.4
450	10	30	24.6	7.7	42.1	33.3
350	30	20	30.2	n.d.	53.8	16.0
450	50	10	33.3	n.d.	42.9	23.8
250	10	30	5.2	0	81.7	13.0
250	10	10	5.3	0	92.9	1.8
250	50	10	22.4	8.4	61.7	15.9
450	10	10	41.6	22.9	56.4	2.0
450	10	30	28.6	10.7	43.8	27.7
250	50	30	20.0	0.8	68.2	11.8
450	10	30	47.1	8.9	42.2	10.8
250	50	10	20.0	0	77.6	1.7
250	10	10	10.5	1.8	88.6	1.0
450	50	10	46.7	14.7	44.8	8.6
450	10	10	41.8	25.1	45.1	13.1

little attention so far. Previous studies merely focused on the use of $ZnCl_2$-KCl and the effects of the salt-to-lignin ratio on product yields and specifically the amounts of phenolic compounds in the liquid product. For example, Kudsy and Kumazawa [15] found that guaiacol was the most abundant phenolic compound produced, which decreased in concentration by increasing the salt-to-lignin ratio (Table 2). With a higher salt-to-lignin ratio, the yields of methanol and phenol also increased, which imply that the salts promote demethoxylation reactions. Moreover, it was found that the formation of phenolic compounds from Kraft lignin pyrolysis in chloride salts had a strong dependence on the amount of salts and that the highest yields of phenolic compounds (except for phenol) were obtained with the lowest concentration of salt used. However, details on the (carbon) yields, product selectivity, and in-depth characterization of the liquid products in molten salt pyrolysis of lignins are still limited. Moreover, detailed studies comparing thermal and molten salt pyrolysis of lignins at similar conditions in the same experimental set-up have not been reported to date.

In this present work, we investigated the pyrolysis of LignoBoost lignin in the presence of a molten salt, that is $ZnCl_2$-KCl-NaCl (mole ratio of 60:20:20) using a gram-scale reactor. This eutectic salt mixture was selected based on its low vapor pressure at high temperature, relatively low melting point (about 200 °C), and good hydrolytic stability [23–29]. The focus of this research was on the liquid pyrolysis product, among others, to optimize the yield and composition. We compared the pyrolysis experiments with and without molten salts to assess the effects of salts on liquid product yield and composition. The physicochemical properties and composition of the products were determined in detail using various analytical techniques. Finally, the recovery and recyclability of the spent salts was assessed using various washing procedures. To the best of our knowledge, such studies including liquid yield optimization and subsequent detailed analysis of the liquids, as well as a proper comparison with thermal pyrolysis have not been reported so far for lignins, and is an absolute novelty of the research described in this paper.

2. Materials and methods

2.1. Chemicals

LignoBoost lignin samples were produced by Innventia, and kindly provided by the Biomass Technology Group (BTG), B.V. (Enschede, The Netherlands). LignoBoost lignin is a purified form of Kraft lignin and contains less ash than Kraft lignin. $ZnCl_2$, NaCl, and KCl salts (analytical purity > 99 %) were purchased from VWR Chemicals (Belgium). Before use, the salts were pre-dried individually by heating them in an oven at 350 °C overnight, following pre-drying protocols recently reported for these salts [23,26]. After cooling, the salts were crushed into fine particles, weighed, and mixed at the required ratio, and stored in a vacuum desiccator. Nitrogen gas was obtained from Linde (> 99.99 % purity). Tetrahydrofuran (THF, anhydrous, ≥ 99.9 %, with 250 ppm BHT as inhibitor), di-n-butyl ether (DBE), and deuterated dimethyl sulfoxide (DMSO-d_6) were purchased from Sigma-Aldrich.

Table 4
Description of the washing procedures used to recover the char and salts from the solid product from the pyrolysis of LignoBoost lignin in molten salts ($ZnCl_2$-KCl-NaCl at 60:20:20 mol ratio).

Washing procedure	Description
Water	Water at 40 °C for 48 h with continuous stirring
Acid 1	1.0 M HCl at 60 °C for 10 min, water at 60 °C, overnight stirring
Acid 2	2.0 M HCl at 60 °C 10 min, water at 60 °C overnight stirring
Acid 1 + Base 1	2.0 M NaOH at 80 °C for 30 min, 1.0 M HCl at 60 °C for 10 min, water at 40 °C, overnight stirring
Acid 2 + Base 1	2.0 M NaOH at 80 °C for 30 min, 2.0 M HCl at 60 °C for 10 min, water at 40 °C, overnight stirring

2.2. Pyrolysis experiments

LignoBoost lignin was pyrolyzed in a gram scale reactor (continuous with respect to N_2 gas and batch with respect to feed), consisting of a gas inlet, pre-heating tube, vessel for lignin and salt, catch pot, and condensers, which were interconnected with metal tubing (Fig. 1) [30,31]. Typically, 1.0 g of lignin sample was mixed with 10.0 g of $ZnCl_2$-KCl-NaCl (eutectic mixture at 60:20:20 mol ratio) inside a quartz tube. The tube was added to the reactor part of the set-up. Subsequently, the reactor was placed in a hot fluidized sand bath to start the pyrolysis process. Temperature profiling experiments (Fig. S1) indicated that it takes about 13–15 min to attain the actual pyrolysis temperature (i.e., 450 °C). A constant flow of N_2 gas was used to transfer pyrolysis vapors from the reactor to the condensers maintained at − 40 °C using a liquid nitrogen-ethanol mixture cooling bath. The mass of the condensable (bio-oil) was determined from the difference in the weight of the tube linings and condensers before and after pyrolysis. The bio-oil was taken from the tube linings and condensers by thoroughly washing with anhydrous THF. The non-condensable gases were collected in a gasbag (SKC Tedlar 3 L sample bag, 9.5″ × 10″ with polypropylene septum fitting) and weighed by water displacement. The mass of the solid product (i.e., char, ash, residues, etc.) excluding the salt was determined from the difference of the weight of the glass tube contents before and after pyrolysis. All product yields are reported as wt% in terms of lignin intake on dry basis.

2.3. Optimization and validation experiments

The effects of process parameters for molten salt pyrolysis such as temperature, reaction time, and N_2 flow rate (independent variables) on responses such as bio-oil, solid, and gas yields were determined. For this purpose, a fractional factorial design with multiple replications was used. A total number of 28 experimental runs were performed and details are given in Table 3. All pyrolysis experiments were performed at least in duplicate and the average product yields are reported.

The data were analyzed using the Design Expert software package. A second order regression model (Eq. 1) was used to optimize responses such as bio-oil yield and conversion. A parameter was considered statistically relevant when the P-value was less than 0.0500. Backward elimination and elimination of outliers was carried out based on diagnostics to improve the model. The optimum reaction conditions based on the mathematical model and surface regression graphs were provided by the software. The resulting mathematical model was validated by performing a pyrolysis experiment in duplicate at the proposed optimum values by the model.

$$Y_i = \beta_0 + \beta_1 x_{i1} + \beta_2 x_{i2} + \cdots + \beta_k x_{ik} + \beta_{11} x_{i1}^2 + \beta_{22} x_{i2}^2 + \ldots + \beta_{kk} x_{ik}^2 + \beta_{12} x_{i1} x_{i2} + \beta_{13} x_{i1} x_{i3} + \ldots + \beta_{k-1,k} x_{i,k-1} x_{ik} + \epsilon_i \quad (1)$$

2.4. Bio-oil and non-condensable gas analysis

The water content of the bio-oils was measured by Karl-Fischer titration using a Metrohm MRD 296 with 702 SM Titrino and 703 Ti stand, following the ASTM E203 standard procedure. About 0.010 g of sample was injected in an isolated glass chamber containing Hydranal Karl-Fischer solvent, and titrations were carried out using the Karl-Fischer titrant Composit 5 K. Triplicate measurements for each sample were conducted and the average value is reported.

Elemental analysis (C, H, N, and S) of the bio-oils was performed using an EuroVector EA3400 Series CHNS-O analyzer with acetanilide as the reference. The oxygen content was determined indirectly by difference. Before elemental analysis of the bio-oils, the THF solvent (used for rinsing the tubes and linings of the reactor) was evaporated until a very viscous to almost dry oil is obtained. All elemental analyses were conducted in duplicate and the average value is reported.

Gas chromatography-mass spectroscopy (GC-MS) analyses were performed on a Hewlett- Packard (HP 6890 series GC system) gas chromatograph equipped with an RTX-1701 capillary column (30 m × 0.25 mm i.d. and 0.25 μm film thickness) and a Quadrupole Hewlett-Packard 6890 mass selective detector. Helium was used as a carrier gas at a flow rate of 2 mL min^{-1}. The injector was set at 280 °C. The oven temperature was kept at 40 °C for 5 min and then increased to 280 °C at a rate of 3 °C min^{-1} and held at 280 °C for 15 min

GC×GC-FID analysis was performed on a trace GC×GC system from Interscience equipped with a cryogenic trap and two capillary columns, i.e., an RTX-1701 capillary column (30 m × 0.25 mm i.d. and 0.25 μm film thickness) connected by a Meltfit to a Rxi-5Sil MS column (120 cm × 0.15 mm i.d. and 0.15 μm film thickness). Quantification of GC×GC main groups of compounds was performed by using an average relative response factor per component group relative to an internal standard (di-n-butylether or DBE). Detailed information on quantification of the amounts of monomers is given in previous papers from our research group [32,33].

The average molecular weights (M_n and M_w) and polydispersity of the bio-oils were determined by gel permeation chromatography (GPC) using an HP1100 equipped with three mixed-e columns (300 × 7.5 mm PL gel, 3 μm) in series using a GBC LC 1240 RI detector. Before GPC analysis, the bio-oil sample was dissolved in anhydrous THF and filtered through a 0.45 μm syringe filter. THF was used as the mobile phase at 1.0 mL min^{-1}, whereas toluene was used as a flow marker. Molecular weights were calibrated against polystyrene standards with known average molecular weights.

^{13}C-nuclear magnetic resonance (NMR) spectra were recorded on a Varian Unity Plus spectrometer (400 MHz) using a 90° pulse and an inverse-gated decoupling sequence with a relaxation delay of 10 s, sweep width of 225 ppm, and 1024 scans. Samples were prepared by dissolving about 100 mg of bio-oil in DMSO-d_6. Heteronuclear single quantum correlation (HSQC) spectra were acquired on a Bruker NMR spectrometer (600 MHz) with the following parameters: 11 ppm sweep width in the F2 domain (^{1}H), 220 ppm sweep width in the F1 domain (^{13}C), 8 scans, 512 increments, and a total acquisition time of approximately 1 h. Sample preparation involved the dissolution of a bio-oil sample in DMSO-d_6.

Gas-phase products were analyzed on a gas chromatograph equipped with a thermal conductivity detector (GC-TCD; Hewlett-Packard 5890 Series II GC equipped with a Poraplot Q Al_2O_3/Na_2SO_4 column and a molecular sieve (5 Å) column). The injector temperature was set at 150 °C and the detector temperature at 90 °C. The oven temperature was kept at 40 °C for 2 min, then heated up to 90 °C at 20 °C min^{-1}, and kept at this temperature for 2 min. A reference gas containing H_2 (55.19 %), CH_4 (19.70 %), CO_2 (18.01 %), CO (3.00 %), propane (1.50 %), ethane (1.49 %), ethylene (0.51 %), and propylene (0.51 %) was used for quantitative analysis.

Table 5
Relevant properties and composition of the LignoBoost lignin feedstock sample.

Property	Value	Property	Value
Moisture content (wt%)	3		
Molecular weights (g mol^{-1})		Organic content (g kg^{-1}) (carbohydrates as anhydrous sugars)	
M_p	3080	Arabinose	2
M_w	4800	Galactose	2
M_n	1260	Glucose	1
Elemental composition (dry basis, wt%)		Xylose	2
C	64.08	Mannose	<1
H	5.91	Acid insoluble residue	953
N	0.03	Acid soluble residue	62
S	1.54	Total lignin	1014
O	29.77	Total carbohydrates	7
Ash content	6 g kg^{-1}	Total amount	1022
HHV	28.02 MJ kg^{-1}		

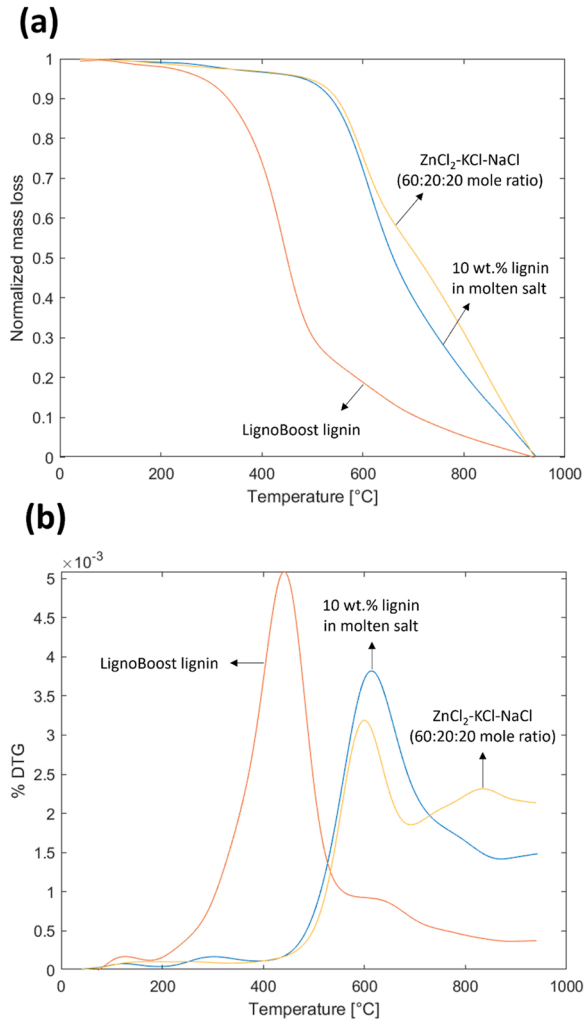

Fig. 2. (a) TGA and (b) DTG curves for a mixture of $ZnCl_2$-KCl-NaCl (60:20:20 mol ratio) and Lignoboost lignin (10 wt%), and the individual components (lignin and salt).

2.5. Analysis of LignoBoost lignin, recovered char, and salts

The moisture content of lignin was determined using a Kern moisture analyzer model DBS 60–3. TGA analyses on lignin, salt and mixtures salt-lignin were performed using a TGA 7 Perkin Elmer instrument. The samples were heated under an N_2 atmosphere at a flow rate of 18 mL min^{-1} and a heating rate of 60 °C min^{-1}, and a temperature ramp of 30–990 °C. Elemental analysis, GPC, and 2D HSQC NMR techniques were also used to analyze the lignin feed (the same instruments were used as described above, see Section 2.4).

Table 6
Comparison of the product yields and elemental composition of the bio-oil obtained from LignoBoost lignin pyrolysis with and without molten salts ($ZnCl_2$-KCl-NaCl at 60:20:20 mol ratio) at 450 °C, 20 mL min^{-1} N_2 flow rate, and 50 min reaction time.

	Lignin-only pyrolysis (no salt)	Lignin pyrolysis in molten salts
Product yields (wt% based on dry lignin intake) ± standard deviation		
Bio-oil	37 ± 1.6	38 ± 1.1
Organics in the bio-oil	20 ± 0.7	21 ± 1.1
% Organics in the bio-oil	54	55
Solid	39 ± 2.1	27 ± 2.7
Non-condensable gas	17 ± 0.9	29 ± 0.9
Mass balance closure (wt %)	93	94
Elemental composition of the bio-oils (wt%, dry basis)		
C	65.34	67.83
H	8.93	10.94
N	n.d.	n.d.
S	0.51	0.12
O	25.22	21.11
H/C	1.64	1.94
O/C	0.29	0.23

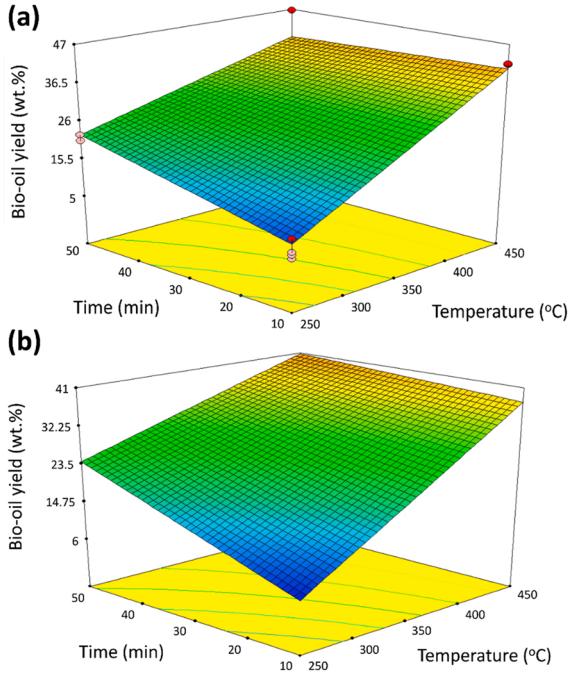

Fig. 3. Response surface plots showing the effects of temperature and reaction time on bio-oil yield for the pyrolysis of LignoBoost lignin in molten salt ($ZnCl_2$-KCl-NaCl at 60:20:20 mol ratio) at a fixed N_2 flow rate of (a) 10 mL min^{-1} and (b) 20 mL min^{-1}.

The solids recovered after reaction ($ZnCl_2$-KCl-NaCl and char) were analyzed by X-ray diffraction (XRD). XRD patterns were collected for a 2θ scan range of 5–80° on a D8 Advanced powder diffractometer (Bruker, Germany) with CuKα radiation (λ = 1.5418 Å) operated at 40 kV and 40 mA. Char and salts were separated from the solid product mixture by adopting various (chemical) treatments involving washing with only water and dilute acid or base and combinations thereof (Table 4). Briefly, water washing consisted of stirring the solid product mixture at 40 °C for 48 h, followed by vacuum filtration, and oven

Table 7
Comparison of product yields, elemental composition and monomer yields of the bio-oil obtained from pyrolysis of LignoBoost lignin with and without molten salts ($ZnCl_2$-KCl-NaCl at 60:20:20 mol ratio) at optimized conditions (450 °C, 10 mL min^{-1} N_2, 10 min).

	Lignin pyrolysis (no salt)	Lignin molten salt pyrolysis
Product yields (wt% based on dry lignin intake) ± standard deviation		
Bio-oil	44 ± 1.2	42 ± 0.9
Organics in the bio-oil	16 ± 1.1	24 ± 0.9
% Organics in the bio-oil	36	57
Solid	50 ± 1.8	51 ± 2.0
Non-condensable gas	7 ± 0.7	8 ± 1.4
Mass balance closure (wt %)	101	101
Elemental composition of the bio-oils (wt%)		
C	63.76	69.24
H	7.75	8.93
N	n.d.	n.d.
S	0.39	0.16
O	28.1	21.67
H/C	1.46	1.55
O/C	0.33	0.23
Monomer yields of the bio-oils (wt% based on dry lignin intake)		
Total monomer	39.5	45.1
Alkylphenolics	27.4	31.3
Aromatics	5.7	9.0

drying (80 °C). A 2.0 M NaOH solution was used for a base washing at 80 °C, whereas a 1.0 or 2.0 M HCl solution was used for washings involving acid at 60 °C. The conditions used for each washing protocol were based on previous research investigating the efficient removal of mineral matter from coal [34]. The recovered chars (i.e., residues) were subsequently analyzed by elemental analysis (CHNS) and XRD.

3. Results and discussion

3.1. Lignoboost lignin characterization

Relevant properties and composition of the Lignoboost lignin used in this study are summarized in Table 5. The moisture content was found to be 3 wt%, the ash content was 0.6 wt%. Syringyl groups were not detected by ^{13}C NMR, consistent with the softwood origin of this lignin.

3.2. TGA analyses of the Lignoboost lignin in the absence and presence of molten salts

TGA analyses were performed under inert conditions (N_2 atmosphere, heating rate of 60 °C min^{-1}) to estimate the most suitable pyrolysis temperature for lignin in the presence and absence of molten salts (Fig. 2). For the lignin sample, an initial weight loss of 3 % up to about 200 °C was observed which is likely mainly due to water evaporation, whereas the steep weight loss (about 60 %) in the 300 °C to 500 °C range is attributed to the decomposition of lignin (the highest devolatilization rate is between about 400 °C and 500 °C). A further progressive but rather limited weight loss is observed at higher temperatures (600–900 °C), which is most likely due to enhanced condensation reactions and/or gasification of the formed carbonaceous material.

For the pure $ZnCl_2$-KCl-NaCl (60:20:20 mol ratio) sample, an initial weight loss of 4 % was observed up to about 400 °C, which is likely due to the release of physisorbed and chemisorbed water upon melting of the eutectic salt. Although all salt samples used were dried prior to use, some external moisture is likely absorbed to the highly hygroscopic salts, for example, during sample preparation for TGA analysis. Progressive weight loss was observed at temperatures > 500 °C, which is most likely due to evaporation of the salt at elevated temperatures.

The TGA/DTG curve for the combination of lignin and $ZnCl_2$-KCl-NaCl differs somewhat from that of lignin in the absence of salt. A small broad peak is present at about 300 °C (DTG, Fig. 4b), which is absent in the lignin only sample, an indication that the maximum rate of pyrolysis vapor formation in the molten salt occurs at a lower temperature than for lignin only. However, due to the relatively low intake of lignin (10 %) in the molten salt, it is difficult to draw a definite conclusion. Nevertheless, the temperature for pyrolysis in molten salt media was selected to be 450 °C (at most) to ensure that salt remains in the liquid phase and is not transferred to the vapor phase by evaporation [23,26], which is a major issue when considering scale up of the technology. In addition HCl formation due to hydrolysis reactions, is also known to be enhanced substantially at higher temperatures [23,26].

3.3. Results for a benchmark pyrolysis experiment using Lignoboost lignin

In the first stage of the experimental work in the gram scale unit (Fig. 1), pyrolysis of the LignoBoost lignin sample without $ZnCl_2$:KCl:NaCl was performed. This benchmark pyrolysis experiment was carried out at a temperature of 450 °C, a N_2 flow rate of 20 mL min^{-1}, a reaction time up to 50 min, and performed in triplicate (average product yields are given in Table 6). After pyrolysis, 37 wt% yield (on dry lignin intake) of a condensed product (bio-oil) was obtained (two phases in the condenser, a dark brown heavy oil phase, and a separate water phase). The amount of organics in the bio-oil was 20 wt% yield based on dry lignin intake. Elemental analysis (dry basis) show the presence of 65 wt % C, 9 wt% H, low levels of S (< 1 wt% total), and 25 wt% O (by difference). The N content of the bio-oils was below the instrument's detection limit. A non-condensable gas phase (17 wt% yield on dry lignin intake) and solid products (i.e., ash, char, residues, etc., 39 wt% yield on dry lignin intake) were also obtained. Based on these data a good mass balance closure of 93 wt% was obtained. The gas-phase was analyzed by GC-TCD and showed the presence of CO_2 (9 wt%), CO (4 wt %), CH_4 (3 wt%), and minor amounts of ethylene, propylene, and propane (1 wt% C2-C3 total).

For comparison, a lignin sample was also pyrolyzed in the presence of $ZnCl_2$-KCl-NaCl (10 wt% lignin in salt) using the same reaction conditions as for the experiment without salts (450 °C, 20 mL min^{-1}, 50 min). After the reaction, a comparable yield of bio-oil was obtained (38 wt% based on dry lignin intake), of which 21 wt% are organics (Table 6). However, the yields of solid (27 wt%) and non-condensable gases (29 wt%) differ considerably from that of the pyrolysis experiment without molten salt and substantially more gas phase components are formed (mass balance closure of 94 wt%). These results suggest that the presence of molten salts under the prevailing pyrolysis conditions promotes formation of gas phase products leading to a reduction in char yields. Remarkably, analysis of the gas products reveals the presence of H_2 (2 wt%) together with CO_2 (15 wt%), CO (6 wt%), and CH_4 and C2-C3 hydrocarbons (both at 3 wt%). Comparison with literature data is not possible as lignin pyrolysis of molten salts is hardly reported (Table 2).

Table 6 summarizes the elemental composition of the bio-oils obtained from lignin pyrolysis with and without molten salts. The bio-oil from molten salt pyrolysis has a lower O content (partially deoxygenated) and a higher C content than that of the lignin feed and the bio-oil from lignin pyrolysis without salt, indicating that the presence of salts leads to higher deoxygenation levels. Furthermore, the S contents of the bio-oils are significantly lower than the original lignin feed as S may also be distributed in other product fractions, i.e., char or gas phase. In earlier work on the micro-pyrolysis of LignoBoost Kraft lignin in $ZnCl_2$-KCl-NaCl, organosulfur compounds were identified (dimethyl sulfide and dimethyl disulfide) in the vapor phase during pyrolysis in the presence of molten salts [26].

3.4. Optimization studies for pyrolysis of LignoBoost lignin in molten salts

The effect of process conditions on the product yields for the pyrolysis of lignin in molten salt was subsequently optimized, and then in a later stage of experimentation, compared with pyrolysis of lignin alone.

Table 8
GC detectable chemical composition of bio-oils obtained from pyrolysis of LignoBoost lignin in the absence and presence of $ZnCl_2$-KCl-NaCl (60:20:20 mol ratio) molten salts at various conditions (semi-quantitative analysis by GC-MS in THF).

Compound	Relative % peak area of components		
	Bio-oil from lignin-only pyrolysis (no salt) (450 °C, 10 mL min^{-1}, 10 min)	Bio-oil from lignin pyrolysis in molten salt (450 °C, 10 mL min^{-1} N_2, 10 min)	Bio-oil from lignin pyrolysis in molten salt (450 °C, 10 mL min^{-1} N_2, 50 min)
Furfural	0.42	-	-
2-Cyclopenten-1-one, 2-methyl	0.12	-	-
Butyrolactone	0.48	-	-
Ethane,1,1-bis(methylthio)	0.12	-	-
2, 4-Dimethylanisole	0.12	-	-
Benzene, 1, 2-dimethoxy	0.29	-	-
P henol, 4-ethyl	0.76	-	-
Phenol, 2-methoxy-3-(2-propenyl)	1.6	-	-
Vanillin	1.78	-	-
Ethanone, 1 -(4 - hydroxy-3 - methoxyphenyl)	2.16	-	-
Benzene	-	-	0.28
Toluene	-	-	1.43
p-Xylene	-	0.58	0.54
Benzene, 1, 3 −dimethyl	-	0.61	0.99
Benzene, 1, 2,4 −trimethyl	-	0.86	-
Benzene, 1, 3,5 −trimethyl		-	0.74
P henol, 2 −ethyl	-	0.68	0.51
P henol, 3 −ethyl	0.23	0.74	0.55
P henol, 3, 5 −dimethyl	-	1.26	1.07
Naphthalene	-	0.57	0.98
P henol, 2-methoxy− 3 −methyl	2.2	-	-
P henol, 2 − methoxy − 4 − methyl−	28.48	1.19	2.91
P henol, 3, 4 − dimethyl−	-	1.03	0.56
Phenol, 2, 4, 6 − trimethyl−	-	0.95	1.23
P henol, 3, 4, 5 −trimethyl	-	1.34	-
P henol, 2, 3, 5 −trimethyl	-	1.2	-
P henol, 2, 3, 5, 6 −tetramethyl	-	0.82	-
P henol, 2 −methyl	1.75	4.82	3.79
P henol, 2, 6 −dimethyl	0.27	1.71	0.94
P henol, 2, 4 −dimethyl	0.37	2.04	1.54
P henol, 2, 3 −dimethyl	1.58	2.23	1.22
P henol, 2, 5 −dimethyl	-	1.75	1.11
1, 2-Benzenediol, 3 −methyl	-	6.65	7.1
P henol, 4 −ethyl− 2methoxy	18.22	3.31	3.59
1, 2 −Benzenediol, 4 −methyl	2.07	5.85	6.22
P henol, 2 −methoxy− 4 −propyl	3.47	2.13	2.19
P henol	2.16	10.5	9.51
P henol, 4 − methyl−	3.21	8.35	6.62
P henol, 2 − methoxy−	23.37	30.29	34.52
1, 2 −Benzenediol	4.95	8.7	9.96
Total peak area (%)	**100**	**100**	**100**

Specifically, the effects of temperature (250–450 °C), N_2 flow rate (10–30 mL min^{-1}), and reaction time (10–50 min) (Table 3) on bio-oil, gas, and solids yields were determined. Experiments were performed at least in duplicate and the average yields are also given in Table 3.

According to the model, the bio-oil yield is strongly affected by temperature and reaction time, whereas the nitrogen flow rate has a lesser effect. The best model for the bio-oil yield is given in Eq. 2.

$$Bio-oil\ yield = -34.33+0.175T-0.686time-0.366flow\ rate-0.00185T \times time+0.01flow\ rate \times time \quad (2)$$

Relevant statistical data in the form of analysis of variance (ANOVA) for bio-oil are summarized in Table S1. The F-value of the model was high (94.63), suggesting that the model is significant and adequately represents the correlations between the response and the variables. Moreover, the P-value of the model is low (1.0×10^{-4}), indicating that the model is statistically significant. Fig. S2 presents a parity plot of the actual or experimental bio-oil yields versus the model predictions, showing that the model bio-oil yields are in good agreement with the experimental ones.

The highest yield of bio-oil obtained is 47.1 wt% based on dry lignin, obtained at 450 °C for 10 min and a N_2 flow rate of 30 mL min^{-1} (Table 3). Fig. 3 shows the effects of temperature and reaction time on bio-oil yield at low and high N_2 flow rates ((a) 10 mL min^{-1} and (b) 20 mL min^{-1}). It is evident from these plots that the yield is strongly affected by the reaction temperature and increasing the temperature to the limit of the design (450 °C) leads to higher bio-oil yields. Fig. S3 shows that at lower temperatures (i.e., about 250–300 °C), solid products dominate. At higher temperatures (i.e., about 400–450 °C), significant amounts of bio-oil are obtained, with a concomitant decrease in solid yields. This trend seems to independent of the N_2 flow rate. The gas yields also increase with temperature (Fig. S4).

Aside from the pyrolysis temperature, the product distribution is also affected, though less pronounced, by the reaction time (Fig. 3). Higher bio-oil yields are obtained when the molten salt pyrolysis experiments are run at prolonged reaction times, though the effects are most pronounced at low temperatures. Finally, it appears that the nitrogen flow rate does not have a major effect on the bio-oil yield, as illustrated by comparing Fig. 3a (10 mL min^{-1}) and b) (20 mL min^{-1}).

Besides the bio-oil yield, the amounts of organics in the oil is highly relevant. The experimental data (Table 3) show that the organic yield varies between 0 and 25.1 wt% (on dry lignin intake). Particularly at the low temperature ion the range (250 °C), the organic yield is very low and the main product is actually water. Data on the effects of process conditions on the yields of organics in the bio-oil (dry basis) are given in

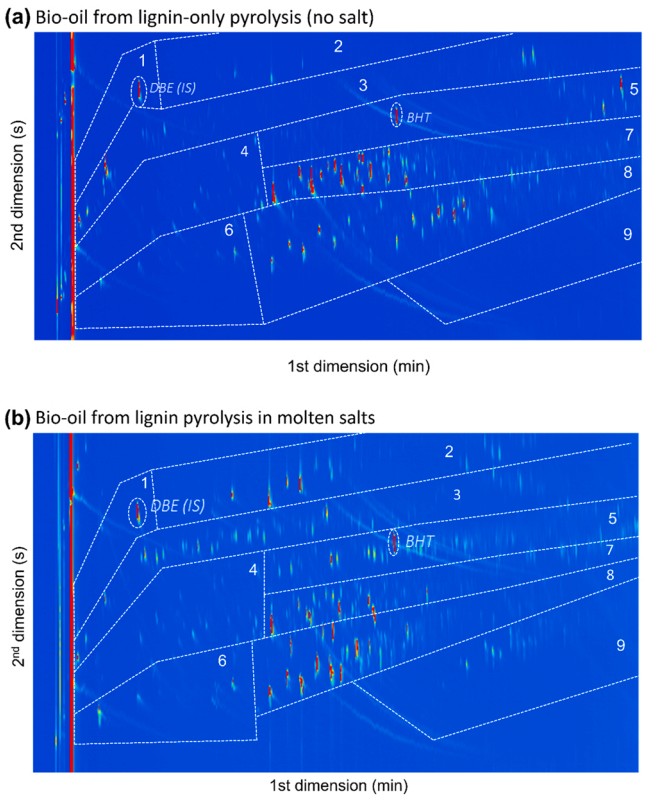

Fig. 4. GC×GC-FID chromatograms of bio-oil from pyrolysis of LignoBoost lignin in the (a) absence and (b) presence of molten salts ($ZnCl_2$-KCl-NaCl at 60:20:20 mol ratio) at optimized conditions (450 °C, 10 min, 10 mL min^{-1} N_2), with indication of various component groups: 1 = cyclic alkanes, 2 = linear/branched alkanes, 3 = aromatics, 4 = ketones/alcohols, 5 = naphthalenes, 6 = volatile fatty acids, 7 = guaiacols, 8 = alkylphenolics, 9 = catechols (DBE or n-dibutylether as internal standard and BHT is a stabilizer in THF).

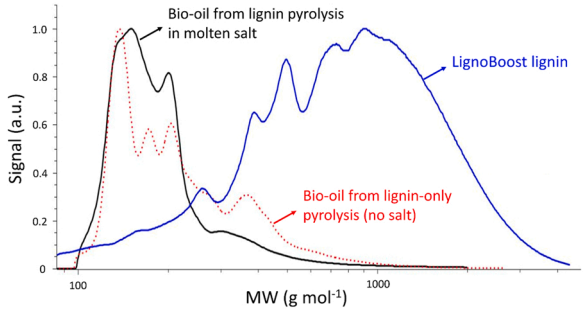

Fig. 5. GPC chromatograms of LignoBoost lignin and the bio-oils obtained from pyrolysis in the absence and presence of molten salts ($ZnCl_2$-KCl-NaCl at 60:20:20 mol ratio) at optimized conditions (450 °C, 10 min, 10 mL min^{-1} N_2).

Table 9
Average molecular weights of LignoBoost lignin and its bio-oils in the absence and presence of molten salts ($ZnCl_2$-KCl-NaCl at 60:20:20 mol ratio) at optimized conditions (450 °C, 10 min, 10 mL min^{-1} N_2).

Sample	M_n (g mol^{-1})	M_w (g mol^{-1})	Polydispersity index
LignoBoost lignin	1260	4800	3.8
Bio-oil from lignin-only pyrolysis (no salt)	200	260	1.3
Bio-oil from pyrolysis of lignin in molten salts	180	210	1.2

Table S2 and visualized in Fig. S5. With this model available, the optimum reaction conditions for the maximum yield of organics in the bio-oil were determined. The highest yield of organics in the bio-oil according to the model is 24 wt% at a temperature of 450 °C, a reaction time of 10 min, and an N_2 flow rate of 10 mL min^{-1} (Fig. S5). Two validation experiments were carried out at these conditions to verify the accuracy of the model. An average yield of 23 wt% organics in the bio-oil was obtained. Thus, the experimental yield is in good agreement with the predicted value from the model.

For comparison, the distribution of products from lignin pyrolysis at the same optimized conditions but in the absence of molten salt was also experimentally determined. As presented in Table 7, the average yields of bio-oil, gas, and solid products are comparable with good mass balance closures (close to 100 %). However, the proportion of organics in the bio-oil obtained from molten salt pyrolysis is significantly higher as compared to the thermal pyrolysis (57 % vs. 36 %). This result further highlights the beneficial effect of using molten salt in obtaining higher amounts of organics in the product bio-oils.

3.5. Characterization of reaction products

3.5.1. Bio-oils

The bio-oils obtained from the pyrolysis experiments performed at optimum conditions (450 °C reaction temperature, 10 mL min^{-1} N_2 flow rate, 10 min reaction time) were characterized in detail (elemental analysis, GC, GPC, and NMR). Table 7 summarizes the elemental analysis data for the bio-oils. The C content of the bio-oil from molten salt pyrolysis is higher than the original lignin sample as well as the bio-oil from lignin pyrolysis without salt. Moreover, the O content is also reduced for the bio-oil in the presence of molten salts, suggesting the occurrence of some deoxygenation reactions during pyrolysis in molten salts.

Information on the chemical composition of the volatile part of the organic fraction of the bio-oils was obtained by GC-MS. Table 8 summarizes the identified components, together with their contents based on relative peak areas. In the absence of molten salts, pyrolysis of lignin at optimum conditions for organics (i.e., 450 °C, 10 mL min^{-1} N_2 flow rate, 10 min reaction time) produced a bio-oil containing significant amounts of phenolic compounds, namely 2-methoxyphenol (23.4 area %), 2-methoxy-4-methylphenol (28.5 area%), and 4-ethylguaiacol (18.2 area%). The presence of these compounds and other phenolics in bio-oil is attributed to the thermal decomposition of lignin structure, which is well-documented in the literature [10,35,36].

In the presence of molten salts (pyrolysis performed under the same reaction conditions at 450 °C, 10 min reaction time, and 10 mL min^{-1} N_2 flow rate), the relative proportion of 2-methoxy-4-methylphenol and 4-ethylguaiacol in bio-oil is considerably reduced (4.5 area%), though more guaiacol is formed (30.3 versus 23.4 area%). When compared to experiments in the absence of salts, more phenol (from 2.2 to 10.5 area %), 4-methylphenol (from 2.2 to 10.5 area%), and catechol (from 5.0 to 8.7 area%) are formed. These findings suggest that 2-methoxy-4-methylphenol and 4-ethylguaiacol are converted to other, less methoxylated species in the presence of molten salts, indicative of catalytic effects of the salts, and particularly on demethoxylation reactions. These findings are in line with the results of previous studies on pyrolysis of Kraft lignin in molten salts (Table 2) [15,26]. An increase in pyrolysis reaction time from 10 min to 50 min (450 °C and 10 mL min^{-1} N_2) resulted in additional deoxygenation towards monoaromatics benzene, toluene, and xylene, and naphthalenes.

To quantify the amounts of the main organic compound classes, the bio-oils obtained from lignin pyrolysis at optimized conditions (450 °C, 10 mL min^{-1} N_2, 10 min) were analyzed using GC×GC-FID. The results are summarized in Table 7 and representative chromatograms are shown in Fig. 4. The total monomer yields in the bio-oil from pyrolysis of lignin with and without molten salts are 45 wt% and 40 wt% (on dry lignin intake), respectively. This result suggests that a significant

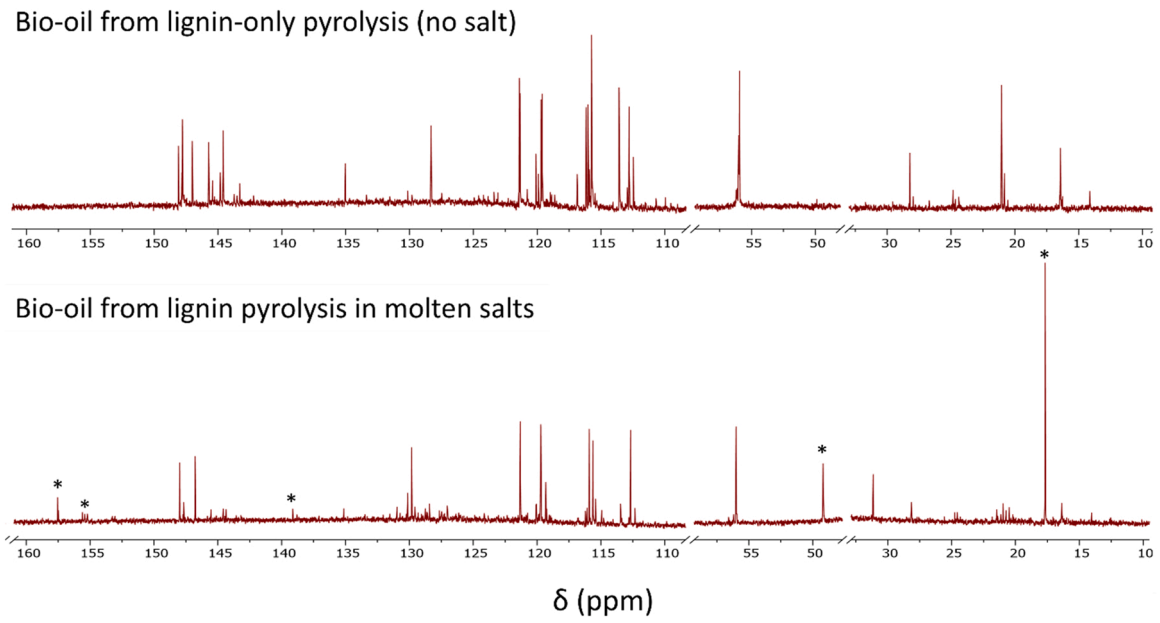

Fig. 6. ^{13}C NMR spectra of bio-oils obtained from pyrolysis of LignoBoost lignin in the absence (top) and presence (bottom) of molten salts ($ZnCl_2$-KCl-NaCl at 60:20:20 mol ratio) at optimized conditions (450 °C, 10 min, 10 mL min^{-1} N_2).

Table 10
^{13}C NMR integrations for specific chemical shift regions for bio-oils obtained from pyrolysis of lignin in the absence and presence of molten salts ($ZnCl_2$-KCl-NaCl at 60:20:20 mol ratio) at optimized conditions (450 °C, 10 min, 10 mL min^{-1} N_2).

Type of carbon	Chemical shift region (ppm)	Relative ^{13}C NMR area (%)	
		Bio-oil from lignin-only pyrolysis (no salt)	Bio-oil from lignin pyrolysis in molten salts
Aliphatic C-C	0–55	15.9	32.5
Methoxy	55–57	5.3	1.7
Aliphatic C-O	57–95	-[a]	-
Aromatic C-H	95–122	9.9	8.1
Aromatic C-C	122–139	36.8	28.6
Aromatic C-O	139–165	32.2	27.5
Carbonyl	165–210	-	1.6

[a]- means not detected.

proportion of the bio-oils is of low molecular weight. Moreover, significantly higher amounts of aromatics, alkylphenolics, and linear/branched alkanes are observed in the bio-oil from lignin pyrolysis in molten salt than in lignin-only pyrolysis as a result of demethoxylation reaction in the presence of salts, as shown above and as shown previously [26].

The GPC chromatograms for lignin and the bio-oils obtained from pyrolysis experiments at optimized conditions (450 °C, 10 min, and 10 mL min^{-1} N_2) are presented in Fig. 5 and the molecular weights are summarized in Table 9. Upon pyrolysis, both in the presence and absence of salts, a substantial reduction of the average molecular weight and polydispersity index of the lignin feed was observed, suggesting depolymerization, with the concomitant formation of low molecular weight components, in line with the GC results. Higher molecular weight compounds (i.e., dimers and oligomers from depolymerization of the individual biopolymers) between about 400–600 g mol^{-1} are also present, as well as higher molecular weight fragments.

Of interest is the observation that the molecular weight reduction in the presence of salts is higher than in the absence of salts. This is particularly evident when considering the higher molecular weight tail, which is significantly reduced when using salts. As such, the salts not only change the composition of the lower molecular weight fraction by demethoxylation, as shown by GC, but also are active as depolymerization catalysts.

Fig. 6 shows the ^{13}C NMR spectra of the bio-oils obtained from lignin pyrolysis in the presence and absence of salts at optimized conditions. Table 10 summarizes the ^{13}C NMR chemical shift ranges and their assignments for various types of carbon present in the bio-oils [37–39]. The amount of carbons in methoxy groups is significantly lower (5.3 %C versus 1.7 %C) in the bio-oil obtained in molten salts, in agreement with GC findings and indicating that salts indeed catalyze the cleavage of methoxy groups. As shown above, demethoxylation reaction on lignin gives alkylated phenols and catechols. The bio-oil from lignin-only pyrolysis contains a significant amount of aromatic carbons (79 %C) and some aliphatic carbons (16 %C). The functionalities that belong to these regions include phenolic structures with methoxy groups and a propyl side chain. On the other hand, the bio-oil from lignin pyrolysis in molten salts shows increased amounts of aliphatic carbons (33 %C). New peaks (as indicated by an asterisk) were found in the region associated with aliphatic and aromatic in C-C and C-O units in bio-oils from molten salt pyrolysis.

The LignoBoost feed and the bio-oil obtained after pyrolysis in molten salts were further characterized by 2D HSQC NMR (Fig. 7, assignments of peaks was taken from references [40–43]). The HSQC spectrum referring to the aromatic units of lignin (Fig. 7(a), red spectrum) at δ_C/δ_H 110–135/6.3–7.7 ppm clearly shows that this particular lignin consists only of guaiacyl units (G), as was expected due to the nature of this lignin (derived from softwood). A ferulate unit (FA) is present to some extent since the C2-H2 and C6-H6 correlation peaks of the ferulate end-groups appear in the spectrum at δ_C/δ_H 112/7.6 ppm (FA_2) and δ_C/δ_H 122/7.3 ppm (FA_6), respectively. There is also a peak at δ_C/δ_H 128/7.0 ppm that corresponds to the β atom of an aldehyde end-group (J_β structure). Lastly, the H structure, which pertains to the $C_{2,6}$-$H_{2,6}$ similar as in *p*-hydroxyphenyl units is also present with its correlation at δ_C/δ_H 130/7.0 ppm. Upon lignin pyrolysis in molten salts (green spectrum), a significant reduction in the amount of G units is observed, indicative for demethoxylation by the catalytic action of salts. The FA and J structures disappeared but the H structure remained. This observation suggests that demethoxylation, C-C bond cleavage, and

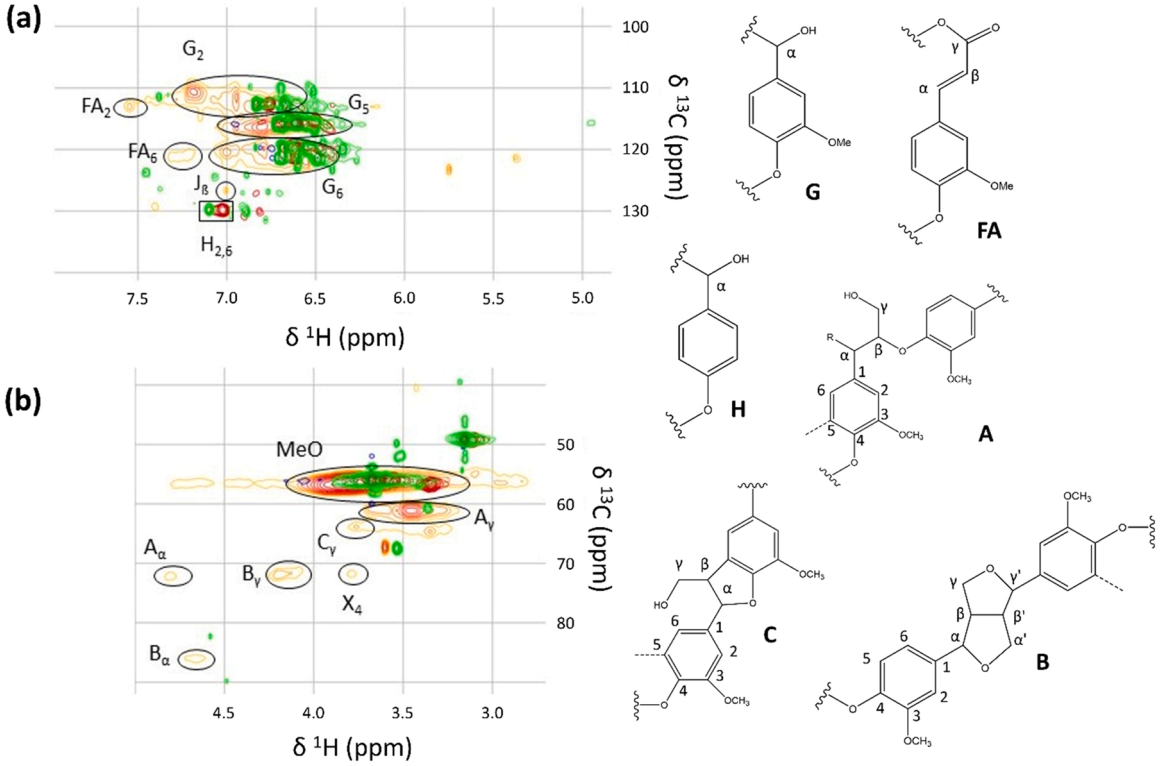

Fig. 7. 2D HSQC NMR spectra of LignoBoost lignin feedstock (red spectrum) and the bio-oil obtained from lignin pyrolysis in $ZnCl_2$-KCl-NaCl (60:20:20 mol ratio) molten salts (green spectrum) showing the (a) aromatic and (b) methoxy regions of the spectra.

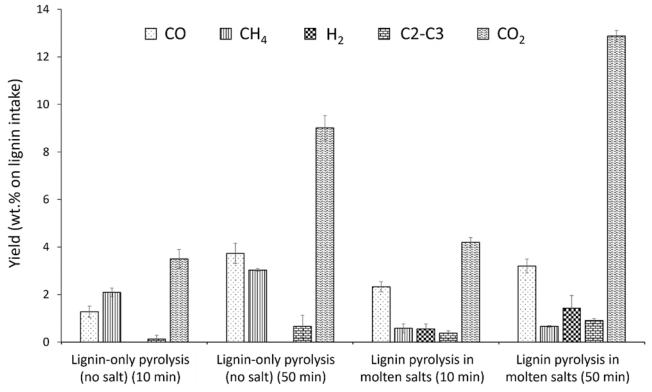

Fig. 8. Yields and composition of non-condensable gases from the pyrolysis of LignoBoost lignin in $ZnCl_2$-KCl-NaCl (60:20:20 mol ratio) molten salts at optimum reaction conditions (450 °C, 10 mL min^{-1}, 10 min) and one at longer reaction time (450 °C, 10 mL min^{-1}, 50 min).

decarbonylation phenomena occurred during lignin pyrolysis in molten salts, leading to monomeric products, i.e., (alkylated) phenols, benzenes, catechols, and potentially gas-phase products.

The part of the HSQC spectrum of the lignin feedstock showing interunit linkages (55–90/2.8–5.0 ppm) (Fig. 7(b), red spectrum) is dominated by strong signals of both the phenylcoumaran structures (β-5′, type C linkages, δ_C/δ_H 56/3.8 ppm) and β -aryl ethers (β -O-4′, type A linkages at δ_C/δ_H 62/3.5 ppm), whereas the pinoresinols or β-β', type B linkages (δ_C/δ_H 72/4.2 ppm) do exist to some extent. Small amounts of xylan were also observed at δ_C/δ_H 72/3.8 ppm (X structure), indicating the presence of some carbohydrate impurities in the starting lignin material. Upon pyrolysis in molten salt (green spectrum), it is clear that these structures (A, B, C, and X) are effectively disrupted, indicating that oligomers are reduced to lower molecular weight and monomeric aromatics.

Table 11
Comparison of the elemental composition of char products recovered from the solid product mixtures during pyrolysis of LignoBoost lignin with and without $ZnCl_2$:KCl:NaCl (60:20:20 mol ratio) molten salts using various adopted washing treatments.

Washing procedure	Elemental composition (wt%)[a]					H/C	O/C
	C	H	N	S	O or O + salts[b]		
Lignin pyrolysis at 450 °C, 10 min, 10 mL min^{-1} without salt and in molten salts							
Without salt	80.03	3.87	0.61	0.90	14.59	0.59	0.14
In molten salts							
Water[c]	64.95	3.45	0.23	0.83	30.54	0.64	0.36
Acid 1[d]	76.71	3.72	0.28	0.89	18.40	0.59	0.18
Acid 2[e]	76.65	3.36	0.30	0.68	19.01	0.53	0.19
Acid 1 + Base 1[f]	75.54	3.30	0.31	0.59	20.26	0.53	0.21
Acid 2 + Base 1[g]	76.13	3.42	0.31	0.58	19.56	0.54	0.2
Lignin pyrolysis at 450 °C, 50 min, 10 mL min^{-1} without salt and in molten salts							
Without salt	80.21	3.95	0.69	1.03	14.12	0.6	0.14
In molten salts							
Water[c]	64.87	3.20	0.29	0.85	30.80	0.6	0.36
Acid 1[d]	77.00	3.81	0.32	0.94	17.94	0.6	0.18
Acid 2[e]	77.15	3.44	0.31	0.73	18.38	0.54	0.18
Acid 1 + Base 1[f]	76.87	3.49	0.38	0.64	18.63	0.55	0.19
Acid 2 + Base 1[g]	77.72	3.51	0.34	0.61	17.84	0.55	0.18

[a] Dry basis. [b] Obtained by difference (100 - CHNS). [c] Water at 40 °C for 48 h. [d] 1.0 M HCl at 60 °C for 10 min, water at 60 °C, overnight stirring. [e] 2.0 M HCl at 60 °C 10 min, water at 60 °C overnight stirring. [f] 2.0 M NaOH at 80 °C for 30 min, 1.0 M HCl at 60 °C for 10 min, water at 40 °C, overnight stirring. [g] 2.0 M NaOH at 80 °C for 30 min, 2.0 M HCl at 60 °C for 10 min, water at 40 °C, overnight stirring.

3.5.2. Composition of the gas phase

Fig. 8 shows the yields and composition of non-condensable gases generated from pyrolysis of LignoBoost lignin at optimum reaction conditions. In the absence of molten salts, pyrolysis for 10 min produced

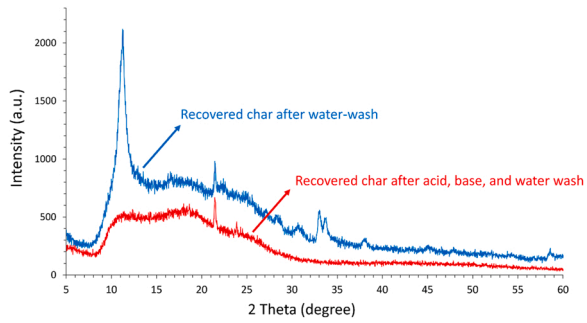

Fig. 9. XRD patterns of the recovered char from the solid products from the pyrolysis of LignoBoost lignin with $ZnCl_2$-KCl-NaCl (60:20:20 mol ratio) using water only (blue) and acid, base, and water (red) washing treatments. (For interpretation of the references to color in this figure legend, the reader is referred to the web version of this article.)

mainly CO and CO_2, suggesting the occurrence of decarbonylation and decarboxylation reactions. Some CH_4 was also detected, which is likely a result of demethoxylation and/or methanation reactions. Propyl side chains contain ether and hydroxyl functionalities that can dehydrate forming alkane, alkene, and carbonyl functionalities. For experiments in the presence of molten salts, also at 10 min, the overall yield of gas-phase products slightly increased. The product selectivity, though, was remarkably different with more H_2 and less CH_4 than found for lignin-only pyrolysis.

At prolonged reaction time (for example, for 50 min) for both thermal pyrolysis and pyrolysis in molten salts, gas formation is promoted and higher amounts of H_2 and CO_2, and to a lesser extent, CO is formed. In comparison to thermal pyrolysis, the gas yield, and particularly the amount of CO_2 in the gas phase is considerably higher for lignin pyrolysis in molten salts.

3.5.3. Solid product characterization

The solid products obtained from pyrolysis of LignoBoost lignin with and without molten salts were characterized in terms of their elemental composition (Table 11) and structure (XRD, Fig. 9). To recover the char from the salts, and to allow for salt recycling in the process, a simple washing procedure was adopted [34], that is, by stirring the solid products continuously in deionized water at 40 °C for 48 h. The C content of the recovered char or residue from molten salt pyrolysis (450 °C, 10 min, 10 mL min^{-1}) is significantly lower as compared to the char from lignin-only pyrolysis (65 vs. 80 wt% C), suggesting that salts are still present in the former. XRD analysis of this residue indeed showed (sharp) peaks likely associated with the salts, suggesting that water-wash only is not completely effective in separating the char from the salts. This observation is also supported by comparing this XRD pattern with the one from the char from lignin-only pyrolysis (no salt), which shows two broad peaks of low intensity indicative of its amorphous nature (Fig. S6; the XRD pattern for the starting salt mixture is shown in Fig. S7).

Thus, it is clear that a simple water wash is not sufficient to remove the salt from the char. As such, the use of extended washing procedures involving acid (1.0 M and 2.0 M HCl then water at 60 °C) and acid and base (1.0 M and 2.0 M HCl at 60 °C, then 2 M NaOH at 80 °C, then water at 40 °C) was tested, as summarized in Table 4. Table 11 shows that the C contents of the recovered char or residue from molten salt pyrolysis after these treatments are more comparable to the C content of the char from lignin-only pyrolysis (76–78 vs. 80 wt% C). These results suggest that such treatments are more effective to recover char and remove salts from the solid products than the water-wash only, though the latter was performed at a lower temperature (40 °C). Efficient removal of salts, for instance, by optimization of the water and acid and base washing procedures, is thought to be key to increase char recovery and recyclability of the spent salts and can be a subject of future investigation. XRD analysis of the recovered char, for example, after acid, base, and water wash of the solid product shows broad peak of low intensity and absence of diffraction peaks attributed to the salt (Fig. 9). Elemental analyses also show that a considerable amounts of N and S containing impurities in the feed are retained in the char.

3.6. Reaction network

Based on the chemical composition (GC-MS NMR) and the molecular weights of the bio-oils (GPC), the gas phase composition (GC-TCD) and solid phase compositions and structure (elemental and XRD analyses), a reaction network for the pyrolysis of LignoBoost lignin in the absence

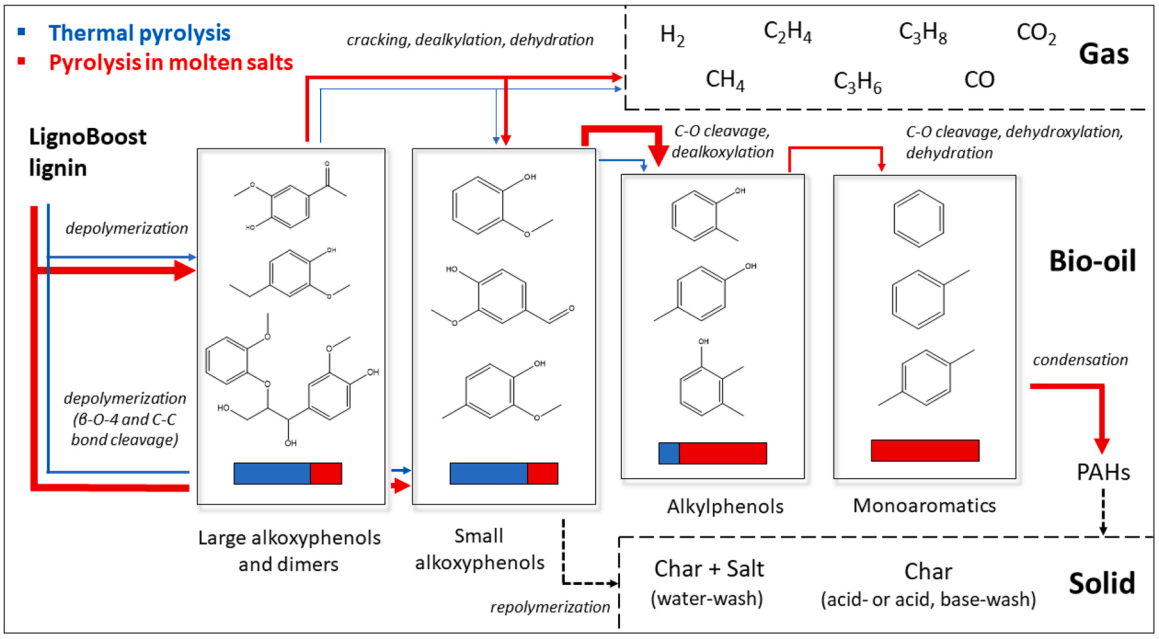

Fig. 10. Proposed general pathways occurring during pyrolysis of LignoBoost lignin in the presence (red arrow) and absence (blue arrows) of molten salts. (For interpretation of the references to color in this figure legend, the reader is referred to the web version of this article.)

(depicted in blue arrows) and presence of molten salts (red arrows) is proposed (Fig. 10).

In thermal pyrolysis of lignin, initial depolymerization of the lignin structure to lower molecular weight fragments occurs. In this step, residual β-O-4 ether linkages are cleaved, while in a later stage, C-C linkages may also be broken. Monomeric alkoxylphenols and higher molecular weight fragments are the main products in the bio-oil and are formed via these depolymerization reactions. Charring occurs to a significant extent by repolymerization reactions between reactive lower molecular weight fragments and already formed monomers.

In the presence of molten salts, depolymerization of lignin occurs to a greater extent during pyrolysis (indicated by the thicker red arrows compared to the blue ones), due to the catalytic action of the salts [44]. Catalytic activity of either metal ions and/or chloride ions may enhance the rate of cracking reactions from phenolics. Moreover, given the extended contact between lignin with metal ions and/or chloride ions present in the eutectic mixtures, secondary reactions can be catalyzed witn the primary pyrolysis vapors (PAHs, char). Moreover, demethoxylation of alkoxylphenols occurs in the presence of salts during pyrolysis, leading to a significant amount of (alkyl) phenols and catechols in the product oil. The presence of methyl benzenes in bio-oil at prolonged reaction times suggests that C-O cleavage and dehydroxylation also occurred due to the catalytic action of salts during pyrolysis.

The methoxy groups are possibly converted to, among others, gas phase components such as H_2, CO, CO_2, and CH_4. Higher yield of gases is a manifestation of secondary reactions and increased level of cracking, again, possibly due to the catalytic action of metal and chloride ions. Char is ultimately formed by the repolymerization of reactive intermediates [36,45,46] for both thermal and molten salt pyrolysis.

The main difference between pyrolysis with and without molten salt is product selectivity, with smaller alkylphenols and monoaromatics being produced in the presence of salts. Apparently, depolymerization and demethoxylation, as well as deoxygenation reactions are catalyzed by these salts. A change in product selectivity, associated with catalytic effects were also reported in refs [15,26].

4. Conclusions

This present work presents an investigation on the pyrolysis of LignoBoost lignin in a representative molten salt (eutectic mixture of $ZnCl_2$-KCl-NaCl at 60:20:20 mol ratio). Product yields were found to strongly depend on the pyrolysis conditions, and particularly temperature. The optimum yield of organics in the bio-oil for molten salt pyrolysis was 24 wt% on dry lignin intake, obtained at 450 °C, 10 mL min^{-1}, and 10 min. The amount of organics in the bio-oil was significantly higher for molten salt pyrolysis as compared to thermal pyrolysis at similar conditions. GC, GPC, and NMR studies on the product oils indicate that the molten salt affects both the composition and molecular weight of the organic fraction. Demethoxylation and extensive depolymerization appear to occur in molten salt pyrolysis, indicating that the salts are catalytically active. These results imply the possibility of exploiting molten salt pyrolysis to preferentially obtain monomeric phenolic compounds. Overall, molten salt pyrolysis can be used to produce organic-rich bio-oils, which can be used as precursor of bio-based chemicals after suitable (catalytic) post-treatments.

CRediT authorship contribution statement

Conception and design of study: **H.C. Genuino, R.H. Venderbosch, H.J. Heeres**. Acquisition of data: **H.C. Genuino, L. Contucci, J. Osorio Velasco, B. Sridharan, E. Wilbers**. Analysis/interpretation of data: **H. C. Genuino, L. Contucci, O. Akin, J.G.M.Winkelman**. Drafting the manuscript: **H.C. Genuino, L. Contucci**. Revising/Finalising the manuscript: **H.C. Genuino, R.H. Venderbosch, H.J. Heeres**.

Declaration of Competing Interest

The authors declare that they have no known competing financial interests or personal relationships that could have appeared to influence the work reported in this paper.

Data availability

Data will be made available on request.

Acknowledgement

This project has received funding from the European Union's Horizon 2020 Research and Innovation Program under grant agreement number 764089. The authors wish to acknowledge the support of the ABC-Salt Consortium members.

Appendix A. Supporting information

Supplementary data associated with this article can be found in the online version at doi:10.1016/j.jaap.2023.106005.

References

[1] Z. Sun, B. Fridrich, A. de Santi, S. Elangovan, K. Barta, Bright side of lignin depolymerization: toward new platform chemicals, Chem. Rev. 118 (2018) 614–678, https://doi.org/10.1021/acs.chemrev.7b00588.
[2] (a) D.S. Bajwa, G. Pourhashem, A.H. Ullah, S.G. Bajwa, A concise review of current lignin production, applications, products and their environmental impact, Ind. Crops Prod. 139 (2019) 111526–111536, https://doi.org/10.1016/j.indcrop.2019.111526;
(b) Z. Strassberger, S. Tanase, G. Rothenberg, The pros and cons of lignin valorisation in an integrated biorefinery, RSC Adv. 4 (2014) 25310–25318.
[3] L. Kouisni, A. Gagné, K. Maki, P. Holt-Hindle, M. Paleologou, LignoForce system for the recovery of lignin from black liquor: feedstock options, odor profile, and product characterization, ACS Sustain. Chem. Eng. 4 (2016) 5152–5159, https://doi.org/10.1021/acssuschemeng.6b00907.
[4] L. Dessbesell, M. Paleologou, M. Leitch, R. Pulkki, C. Xu, Global lignin supply overview and kraft lignin potential as an alternative for petroleum-based polymers, Renew. Sustain. Energy Rev. 123 (2020), 109768, https://doi.org/10.1016/j.rser.2020.109768.
[5] W. Li, N. Wanninayake, X. Gao, M. Li, Y. Pu, D.-Y. Kim, A.J. Ragauskas, J. Shi, Mechanistic insights into lignin slow pyrolysis by linking pyrolysis chemistry and carbon material properties, ACS Sustain. Chem. Eng. 8 (2020) 15843–15854, https://doi.org/10.1021/acssuschemeng.0c03423.
[6] D.J. Nowakowski, A.V. Bridgwater, D.C. Elliott, D. Meier, P. de Wild, Lignin pyrolysis: results from an international collaboration, J. Anal. Appl. Pyrolysis 88 (2010) 53–72, https://doi.org/10.1016/j.jaap.2010.02.009.
[7] A.R. Ardiyanti, A. Gutierrez, M.L. Honkela, A.O.I. Krause, H.J. Heeres, Hydrotreatment of wood-based pyrolysis oil using zirconia-supported mono- and bimetallic (Pt, Pd, Rh) catalysts, Appl. Catal. A. 407 (2011) 56–66, https://doi.org/10.1016/j.apcata.2011.08.024.
[8] R.H. Venderbosch, A critical view on catalytic pyrolysis of biomass, ChemSusChem 8 (2015) 1306–1316, https://doi.org/10.1002/cssc.201500115.
[9] G. Yildiz, F. Ronsse, R. van Duren, W. Prins, Challenges in the design and operation of processes for catalytic fast pyrolysis of woody biomass, Renew. Sustain. Energy Rev. 57 (2016) 1596–1610, https://doi.org/10.1016/j.rser.2015.12.202.
[10] P.J. Wild, D., W.J.J. Huijgen, H.J. Heeres, Pyrolysis of wheat straw-derived organosolv lignin, J. Anal. Appl. Pyrol. 93 (2012) 95–103, https://doi.org/10.1016/j.jaap.2011.10.002.
[11] S. Guo, J. Zhang, W. Wu, W. Zhou, Corrosion in the molten fluoride and chloride salts and materials development for nuclear applications, Prog. Mater. Sci. 97 (2018) 448–487, https://doi.org/10.1016/j.pmatsci.2018.05.003.
[12] K. Vignarooban, X. Xu, K. Wang, E.E. Molina, P. Li, D. Gervasio, A.M. Kannan, Vapor pressure and corrosivity of ternary metal-chloride molten-salt based heat transfer fluids for use in concentrating solar power systems, Appl. Energy 159 (2015) 206–213, https://doi.org/10.1016/j.apenergy.2015.08.131.
[13] E. Sada, H. Kumazawa, M. Kudsy, Pyrolysis of lignins in molten salt media, Ind. Eng. Chem. Res. 31 (1992) 612–616, https://doi.org/10.1021/ie00002a025.
[14] M. Kudsy, H. Kumazawa, Pyrolysis of kraft lignin in the presence of molten $ZnCl_2$-KCl mixture, Can. J. Chem. Eng. 77 (6) (1999) 1176–1184, https://doi.org/10.1002/cjce.5450770614.
[15] M. Kudsy, H. Kumazawa, E. Sada, Pyrolysis of kraft lignin in molten $ZnCl_2$-KCl media with tetralin vapor addition, Can. J. Chem. Eng. 73 (1995) 411–415, https://doi.org/10.1002/cjce.5450730319.
[16] H. Jiang, N. Ai, M. Wang, D. Ji, A. Ji, Experimental study on thermal pyrolysis of biomass in molten salt media, Electrochemistry 77 (2009) 730–735, https://doi.org/10.5796/electrochemistry.77.730.

[17] A. Yasunishi, Y. Tada, Wood pyrolysis in molten-salt, Kagaku Kogaku Ronbunshu 11 (1985) 346–349.
[18] H.S. Nygård, E. Olsen, Effect of salt composition and temperature on the thermal behavior of beech wood in molten salt pyrolysis, Energy Procedia 58 (2014) 221–228, https://doi.org/10.1016/j.egypro.2014.10.432.
[19] H.S. Nygård, E. Olsen, Molten salt pyrolysis of milled beech wood using an electrostatic precipitator for oil collection, AIMS Energy 3 (2015) 284–296, https://doi.org/10.3934/energy.2015.3.284.
[20] J.K. Maund, D.M. Earp, Fuels from biomass by conversion in molten salts. Research in Thermochemical Biomass Conversion, Springer, Dordrecht, 1988, pp. 542–556.
[21] H.S. Nygård, F. Danielsen, E. Olsen, Thermal history of wood particles in molten salt pyrolysis, Energy Fuels 26 (2012) 6419–6425, https://doi.org/10.1021/ef301121j.
[22] R. Dutta, J.P. Dittami, Molten salt pyrolysis for bio-oil and chemicals, Google Patents, PCT US2016 041063.
[23] N. Sepideh, E. Olsen, H.S. Nygård, Hydrolysis of eutectic compositions in the $ZnCl_2$:KCl:NaCl ternary system and effect of adding ZnO, J. Mol. Liq. 317 (2020) 114069–114076, https://doi.org/10.1016/j.molliq.2020.114069.
[24] W.P. Scarrah, Molten salt hydrocracking of lignite. Screening of viscosity reducers and hydrogen sources, Ind. Eng. Chem. Res. 19 (1980) 442–446, https://doi.org/10.1021/i360075a029.
[25] B. Sridharan, H.C. Genuino, D. Jardan, E. Wilbers, H.H. Van De Bovenkamp, H. J. Heeres, Novel route to produce hydrocarbons from woody biomass using molten salts, Energy Fuels 36 (2022) 12628–12640, https://doi.org/10.1021/acs.energyfuels.2c02044.
[26] A. Estrada Leon, M. Pala, H.J. Heeres, W. Prins, F. Ronsse, Micropyrolysis of various lignocellulosic biomasses in molten chloride salts, J. Anal. Appl. Pyrol. 168 (2022), 105739, https://doi.org/10.1016/j.jaap.2022.105739.
[27] K. Nitta, T. Nohira, R. Hagiwara, M. Majima, S. Inazawa, Physicochemical properties of $ZnCl_2$-NaCl-KCl eutectic melt, Electrochim. Acta 54 (2009) 4898–4902, https://doi.org/10.1016/j.electacta.2009.03.079.
[28] K. Vignarooban, X. Xu, K. Wang, E.E. Molina, P. Li, D. Gervasio, A.M. Kannan, Vapor pressure and corrosivity of ternary metal-chloride molten-salt based heat transfer fluids for use in concentrating solar power systems, Appl. Energy 159 (2015) 206–213, https://doi.org/10.1016/j.apenergy.2015.08.131.
[29] X. Xu, G. Dehghani, J. Ning, P. Li, Basic properties of eutectic chloride salts NaCl-KCl$ZnCl_2$ and NaCl-KCl-$MgCl_2$ as HTFs and thermal storage media measured using simultaneous DSC-TGA, Sol. Energy 162 (2018) 431–441, https://doi.org/10.1016/j.solener.2018.01.067.
[30] H.C. Genuino, I. Muizebelt, A. Heeres, N.J. Schenk, J.G.M. Winkelman, H. J. Heeres, An improved catalytic pyrolysis concept for renewable aromatics from biomass involving a recycling strategy for co-produced polycyclic aromatic hydrocarbons, Green Chem. 21 (2019) 3802–3806, https://doi.org/10.1039/C9GC01485C.
[31] R.C. Tanquilut, H.C. Genuino, E. Wilbers, R.M.C. Amongo, D.C. Suministrado, K. F. Yaptenco, M.M. Elauria, J.C. Elauria, H.J. Heeres, Biorefining of pigeon pea: Residue conversion by pyrolysis, Energies 13 (2020) 2778–2796, https://doi.org/10.3390/en13112778.
[32] I. Hita, H.J. Heeres, P.J. Deuss, Insights into structure-reactivity relationships for the iron-catalyzed hydrotreatment of technical lignins, Bioresour. Technol. 267 (2018) 93–101, https://doi.org/10.1016/j.biortech.2018.07.028.
[33] R.K. Chowdari, S. Agarwal, H.J. Heeres, Hydrotreatment of kraft lignin to alkylphenolics and aromatics using Ni, Mo, and W phosphides supported on activated carbon, ACS Sustain. Chem. Eng. 7 (2019) 2044–2055, https://doi.org/10.1021/acssuschemeng.8b04411.
[34] Z.Y. Wang, Y. Ohtsuka, A. Tomita, Removal of mineral matter from coal by alkali treatment, Fuel Proc. Technol. 13 (1986) 279–289, https://doi.org/10.1016/0378-3820(86)90036-6.
[35] R. Parthasarathi, R. Romero, R.A. Gnanakaran, Theoretical study of the remarkably diverse linkages in lignin, J. Phys. Chem. Lett. 2 (2011) 2660–2666, https://doi.org/10.1021/jz201201q.
[36] L. Du, Z. Wang, S. Li, W. Song, W. Lin, A comparison of monomeric phenols produced from lignin by fast pyrolysis and hydrothermal conversions, Int. J. Chem. React. Eng. 11 (2013) 1–11, https://doi.org/10.1515/ijcre-2012-0085.
[37] J. Hu, R. Xiao, D. Shen, H. Zhang, Structural analysis of lignin residue from black liquor and its thermal performance in thermogravimetric-Fourier transform infrared spectroscopy, Bioresour. Technol. 128 (2013) 633–639, https://doi.org/10.1016/j.biortech.2012.10.148.
[38] A. Kloekhorst, H.J. Heeres, Catalytic hydrotreatment of Alcell lignin fractions using a Ru/C catalyst, Catal. Sci. Technol. 6 (2016) 7053–7067, https://doi.org/10.1039/C6CY00523C.
[39] M.B. Figueiredo, R.H. Venderbosch, P.J. Deuss, H.J. Heeres, A two-step approach for the conversion of technical lignins to biofuels, Adv. Sustain. Syst. 4 (2020) 1900147–1900159, https://doi.org/10.1002/adsu.201900147.
[40] C. Crestini, H. Lange, M. Sette, D.S. Argyropoulos, On the structure of softwood kraft lignin, Green Chem. 19 (2017) 4104–4121, https://doi.org/10.1039/C7GC01812F.
[41] J.L. Wen, S.L. Sun, B.L. Xue, R.C. Sun, Recent advances in characterization of lignin polymer by solution-state nuclear magnetic resonance (NMR) methodology, Materials 6 (2013) 359–391, https://doi.org/10.3390/ma6010359.
[42] T.-Q. Yuan, S.-N. Sun, F. Xu, R.-C. Sun, Characterization of lignin structures and lignin-carbohydrate complex (LCC) linkages by quantitative ^{13}C and 2D HSQC NMR spectroscopy, J. Agric. Food Chem. 59 (2011) 10604–10614, https://doi.org/10.1021/jf2031549.
[43] T.-Q. Yuan, F. Xu, R.-C. Sun, Role of lignin in a biorefinery: separation characterization and valorization, J. Chem. Technol. Biotechnol. 88 (2013) 346–352, https://doi.org/10.1002/jctb.3996.
[44] W. Wang, R. Lemaire, A. Bensakhria, D. Luart, Review on the catalytic effects of alkali and alkaline earth metals (AAEMs) including sodium, potassium, calcium and magnesium on the pyrolysis of lignocellulosic biomass and on the co-pyrolysis of coal with biomass, J. Anal. Appl. Pyrol. 163 (2022) 105479–105511, https://doi.org/10.1016/j.jaap.2022.105479.
[45] K. Wang, K.H. Kim, R.C. Brown, Catalytic pyrolysis of individual components of lignocellulosic biomass, Green Chem. 16 (2014) 727–735, https://doi.org/10.1039/C3GC41288A.
[46] V.B.F. Custodis, S.A. Karakoulia, K.S. Triantafyllidis, J.A. van Bokhoven, Catalytic fast pyrolysis of lignin over high-surface-area mesoporous aluminosilicates: effect of porosity and acidity, ChemSusChem 9 (2016) 1134–1145, https://doi.org/10.1002/cssc.201600105.